Journal of Orthopaedic Translation 21 (2020) 49–56

Contents lists available at ScienceDirect

Journal of Orthopaedic Translation

journal homepage: www.journals.elsevier.com/journal-of-orthopaedic-translation

Original Article

Comparison of bone surface and trough fixation on bone–tendon healing in a rabbit patella–patellar tendon injury model

Muzhi Li [a,b,c,1], Yifu Tang [a,b,c,1], Can Chen [a,b,c], Jiefu Zhou [a,b,c], Cheng Zheng [d], Huabin Chen [a,b,c], Hongbin Lu [a,b,c], Jin Qu [a,b,c,*]

[a] Department of Sports Medicine & Research Centre of Sports Medicine, Xiangya Hospital, Central South University, Changsha, China
[b] Key Laboratory of Organ Injury, Aging and Regenerative Medicine of Hunan Province, Changsha, China
[c] Xiangya Hospital-International Chinese Musculoskeletal Research Society Sports Medicine Research Centre, Central South University, Changsha, China
[d] Department of Orthopaedics, Hospital of Wuhan Sports University, Wuhan Sports University, Wuhan, China

ARTICLE INFO

Keywords:
Bone surface fixation
Bone–tendon healing
Bone–tendon interface
Bone tunnel/trough fixation
Partial patellectomy

ABSTRACT

Background: Many orthopedic surgical procedures involve reattachment between tendon and bone. Whether bone–tendon healing is better facilitated by tendon fixation on a bone surface or within a tunnel is unknown. The purpose of this study was to comparatively evaluate the effects of bone surface versus bone trough fixation on bone–tendon healing in a rabbit patella–patellar tendon (PPT) injury model.

Methods: The rabbits underwent partial patellectomy with patellar-tendon fixation on the osteotomy surface (bone surface fixation, BSF group) (n = 28) or within a bone trough (bone trough fixation, BTF group) (n = 28). The PPT interface was evaluated by macroscopic observation, micro-computed tomography scanning, histological analysis, and biomechanical testing at postoperative week 8 or week 16.

Results: Macroscopically, no signs of infection or osteoarthritis were observed, and the regenerated tissue bridging the residual patella and patellar tendon showed no obvious difference between the two groups. There were significantly higher bone mineral density and trabecular thickness in BSF group compared with BTF group at week 8 ($p < 0.05$ for both). However, the bone volume fraction (BVF), bone mineral density and trabecular thickness in BSF group were significantly lower than those in BTF group ($p < 0.05$ for all) at week 16. Histological analysis demonstrated that new bone was formed at the proximal patella and reattached to the residual patellar tendon through a regenerated fibrocartilage-like tissue in both groups. There was more formation and better remodelling of fibrocartilage-like tissue in BTF group than BSF group at week 8 and week 16 ($p < 0.05$ for both). Biomechanical testing revealed that there was higher failure load and stiffness at the PPT interface in BTF group than BSF group at week 16 ($p < 0.05$ for both).

Conclusions: These results suggested that raptured tendon fixation in a bone trough resulted in superior bone–tendon healing in comparison with tendon fixation on bone surface in a rabbit PPT injury model.

The translational potential of this article: Although the structural and functional difference of knee joint between human and rabbit limit the results to be directly used in clinical, our research does offer a valuable reference for the improvement of reattachment between bone and tendon.

Introduction

Musculoskeletal system functions through the coordination of multiple types of connective tissues. Among them, a specialised transition tissue, called bone–tendon interface (BTI), integrates tendon to bone and serves to facilitate joint motion [1–3]. This specialised interface shows a spatial gradient in composition, structure, and mechanical properties, thus can effectively transfer loading between mechanically dissimilar tissues, such as from tendon/ligament to bone [1–4]. Histologically, typical BTI is composed of four distinct yet continuous tissues: bone, calcified fibrocartilage, noncalcified fibrocartilage, and tendon [1,2,5,6], which ensure its unique function but also increase the difficulty of

* Corresponding author. No 87, Xiangya Road, Xiangya Hospital, Central South University, Changsha, 410008, China.
E-mail address: jinqu@outlook.com (J. Qu).
[1] Muzhi Li and Yifu Tang were co-first authors.

https://doi.org/10.1016/j.jot.2019.12.007
Received 14 May 2019; Received in revised form 9 December 2019; Accepted 13 December 2019
Available online 18 January 2020
2214-031X/© 2019 The Author(s). Published by Elsevier (Singapore) Pte Ltd on behalf of Chinese Speaking Orthopaedic Society. This is an open access article under the CC BY-NC-ND license (http://creativecommons.org/licenses/by-nc-nd/4.0/).

treating injured BTI. Currently, BTI injuries are very common in orthopedics, whereas its healing is much slower when compared with bone fracture or tendon rapture [5,7,8]. The reasons for this complicated healing are that: (1) the healing takes place between soft tendinous tissue and hard bony tissue; (2) the avascularity of injury site impede the healing process; (3) the healing occurs through the formation of fibrovascular scar tissue rather than through the regeneration of a fibrocartilaginous junction in general [5,9,10]. Therefore, promoting the functional and biological recovery of BTI is meaningful and urgent in sports medicine.

Clinically, surgical integrity is the common way for treating BTI injuries, such as reattaching the injured tendon/ligament to bone in rotator cuff repair and anterior talofibular ligament reconstruction [3,11,12]. Based on the fixation site of the tendon, the surgical protocols used to integrate the raptured tendon with the bone could be classified into two categories: direct fixation to the bone surface (bone surface fixation, BSF) and placement within a bone tunnel/trough (bone trough/tunnel fixation, BTF) [13–16]. Compared with bone tunnel/-trough fixation, bone surface fixation is more fit in with the normal anatomy, which directly sutures the tendon torn end to its original bony insertion site without creating a bone tunnel/trough to accommodate the tendon, thus it avoids additional surgical trauma and perturbation on joint kinematics [16]. Correspondingly, BTF may show some superiority in promoting bone–tendon (B–T) healing through other mechanisms. BTF offers a larger contact area between bone and tendon, which stabilises bone–tendon reattachment and guarantees a stabler environment for repair site. Moreover, placement in a bone tunnel/-trough would facilitate infiltration of mesenchymal stem cells (MSCs), which is considered as the main cells in charge of B–T healing and has been reported to effectively enhance osteointegration of tendon grafts in rabbits [16,17]. Besides, the two fixation methods make the BTI healing in two different mechanical environments, which is considered an important factor in cell differentiation and extracellular matrix remodelling. Collectively, the two fixation methods may result in different B–T healing qualities.

To find out the better surgery protocol, this study was designed to comparatively evaluate bone surface versus bone trough fixation on B–T healing, with respect to micro-computed tomography (micro-CT), histomorphology, and biomechanical properties in a rabbit patella–patellar tendon (PPT) injury model.

Materials and methods

Experimental design

The animal ethics committee of our university approved the protocol of this study (Permit No. 2015-06-14). A total of 56 healthy mature male New Zealand rabbits (weight, 3.4 ± 0.3 kg) were involved in this study. They were randomly assigned to the following two groups (n = 28): BSF group and BTF group, to accept different surgical protocols for reattachment of bone and raptured tendon. Animals were sacrificed at 8 and 16 weeks after surgery (14 animals/group/time point) to harvest the quadriceps–patella–patellar tendon–tibia complexes (QPPTCs). After macroscopic observations, six specimens per group per time point underwent micro-CT scanning and histological evaluations, whereas the other 8 specimens were evaluated via biomechanical testing. The number of rabbits required for micro-CT analysis, histological evaluations, immunohistochemistry, and biomechanical testing was determined by power analysis.

Animal model and surgery

Illustration of operation protocols were briefly presented in the Fig. 1. After anaesthetised with 3% sodium pentobarbital (0.8 mL/kg intravenous injection; Sigma), an anterolateral skin incision was longitudinally made on rabbits' right hindlimb knee to expose the patella, patellar tendon, and tibial tuberosity. To normalise the variation of knee kinematics and mechanical loading environment among individuals, surgeries were carefully carried out to ensure a similar PPT interface length. The position of transverse osteotomy was performed between the proximal two-thirds and the distal one-third of the patella in the BSF group (Fig. 1A), whereas, in the BTF group, transverse osteotomy was performed between the proximal three-fourths and the distal one-fourths of the patella (Fig. 1B). After the distal patella and adherent fibrocartilage layer were removed, two evenly spaced tunnels (0.8-mm diameter) were drilled longitudinally through the remaining patella. For animals

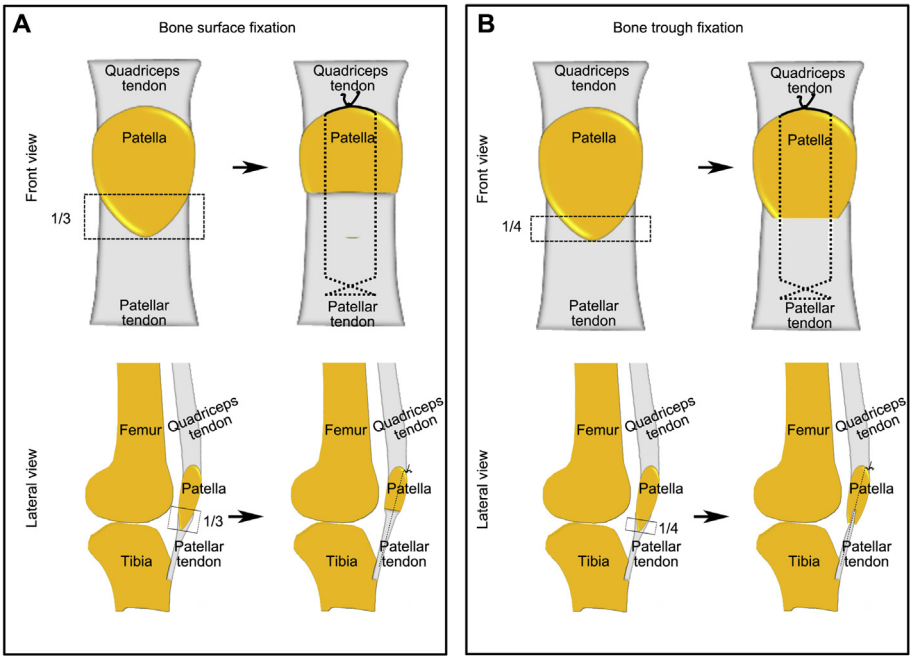

Figure 1. (A) Illustration of bone surface fixation from superior and sagittal view; (B) illustration of bone trough fixation from superior and sagittal view.

randomised to BTF group, a 2-mm-deep and 1-mm-wide bone trough was coronally excavated at the entrance position of the two bone tunnels. The patellar tendons of both groups were then directly sutured to the remaining proximal patella via the two predrilled tunnels with 3–0 nonabsorbable PDS II suture (Ethicon) (Fig. 1). The difference was that the patellar tendon end in the BTF group was inserted into the bone trough of the residual patella. After the suture was tightly tied at the superior pole of the patella, a figure-of-8 tension band wire was additionally drawn around the superior pole of the patella and tibia to protect the surgical site. After closing the surgical incision, cast immobilisation was used for the first 4 weeks and 3-day painkiller (intravenous injection, 1.5 mg/kg per 12 h) (tramadol; Grunenthal GmbH) was given after operation. Rabbits were allowed free cage activities after operation.

Macroscopic observations

The harvest QPPTCs were photographed by a digital camera (60D, Cannon, Japan) for gross evaluation.

Micro-CT scanning

Twenty-four QPPTCs were fixed in 4% neutral buffered formalin and then washed with 0.9% saline to remove the residual formalin. After the other tissues of QPPTCs were carefully dissected to ensure only the PPT interface and attached quadriceps tendon left and then they were scanned by micro-CT (μCT 100; Scanco Medical) with 20-μm voxel size. Scanning data of each specimen were then processed with a 3D Gaussian filter and a global threshold to extract bone from soft tissue or bone marrow for subsequent analysis. The new bone at the PPT healing interface was separated from the remaining patella. Morphological parameters of the new bone were calculated, including bone volume fraction (BVF), bone mineral density (BMD), trabecular thickness (Tb.Th) and trabecular number (Tb.N).

Histological analysis

After micro-CT analysis, the fixed specimens were decalcified with a 1-to-1 mixture of 20% sodium citrate and 50% formic acid and then embedded in paraffin. Serial 5 μm-thick sections from the midsagittal plane of each specimen were cut by a microtome (Leica RM2125; Reichert-Jung GmbH) and then stained with hematoxylin & eosin (H&E), toluidine blue/fast green (TB/FG) or Sirius Red (SR). For accurate comparisons between groups, all histological images were captured under exactly the same conditions of parameter settings by a transmitted light microscope (CX31; Olympus) or a polarised microscope (Eclipse CI; Nikon). The captured images were imported to Image-Pro Plus (version 6.0.0; Media Cybernetics Inc) for semiquantitative assessments by 2 independent investigators. H&E stained sections were used to exhibit histological characteristics of repaired PPT interface. TB/FG stained section were used to calculate fibrochondrocytes density and proteoglycans accumulated in the regenerated fibrocartilage layer through an established protocol [5,10]. The integrated optical density of the fibrocartilage staining by TB/FG was measured to evaluate its proteoglycan content. Meanwhile, SR staining sections were captured by polarised microscope to quantify the collagen alignment and maturation at the regenerated fibrocartilage in accordance with the published literature [5,18]. All of the data analyses were performed by the same person on the investigational team (C.C and J. Z).

The expression of osteogenic marker RUNX2 and chondrogenic marker SOX9 at PPT interface were evaluated by immunohistochemistry. After dewaxed by xylene and rehydrated by ethanol, the tissue sections were boiled in 10-mM citrate buffer (pH = 6.0) in a microwave oven at 600 W for 15 min to retrieve antigens. The sections were cooled to room temperature, washed twice with phosphate buffer solution (PBS), incubated with 3% hydrogen peroxide for 10 min to block endogenous peroxidase activity, and then incubated with 3% bull serum albumin (BSA) for 45 min at room temperature. The processed sections were incubated with anti-RUNX2 (1:100, bs-1134R; Bioss, Beijing, China) or anti-SOX9 (1:100, bs-4177R; Bioss, Beijing, China) antibody, respectively overnight at 4 °C. After washed twice with PBS, the sections were incubated with biotinylated secondary antibody for 1 h at 37 °C and then incubated with HRP-streptavidin for 15 min. All immunohistochemistry images were captured by a transmitted light microscope (CX31; Olympus).

Biomechanical testing

Biomechanical testing were used as the ultimate index to assess the healing quality of PPT interface, which was measured by a mechanical testing machine (MTS insight, MTS Systems Corp, USA) (Fig. 6A). Briefly, after 32 QPPTCs were thawed overnight at 4 °C, the periarticular connective soft tissues, the suture material, and tension band wire were carefully dissected. Then, the QPPTC was loaded to failure at a rate of 20 mm/min after a preload of 1 N. Failure load (N) and stiffness (N/mm) was obtained from the recorded load–displacement curve. During testing, 0.9% saline was applied to avoid dehydration of the specimens.

Statistical analysis

Statistical analyses were performed using SPSS 18.0 software (SPSS Inc). All quantitative data were expressed as mean ± SD, and differences between the two groups were evaluated using one-way analysis of variance (ANOVA). Statistical significance was set at $p < 0.05$.

Results

Macroscopic observations

No decrease in knee joint motion after surgery was discovered. No animal was lost during or subsequent to surgery. Macroscopically (Fig. 2), all of the harvested QPPTCs showed no signs of infection and osteoarthritis. Fibrous reaction was found near the PPT healing site, and a regenerated tissue was bridging the residual patella and patellar tendon in the two groups. No obvious differences between the two groups were observed on gross inspection.

Micro-CT evaluation

In accordance with the micro-CT images, new bone gradually formed at the PPT healing site from postoperative week 8–16 in both BSF and

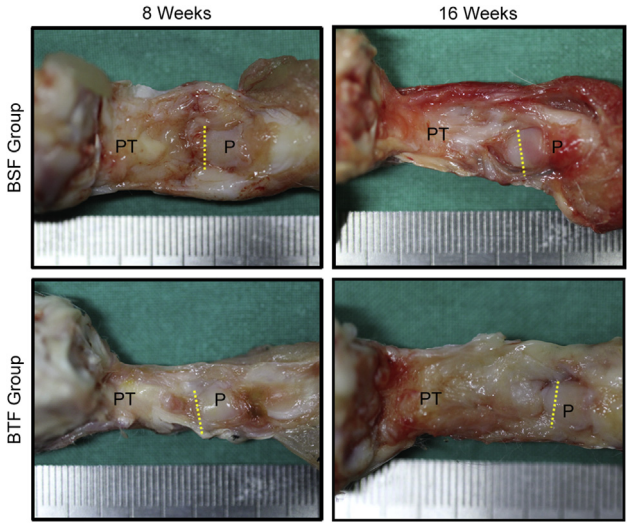

Figure 2. Gross observation of the QPPTCs in BSF and BTF groups at postoperative week 8 or 16. Yellow dashed line indicates osteotomy site. PT, Patellar tendon, P: Patella; QPPTCs, Quadriceps–patella–patellar tendon–tibia complexes.

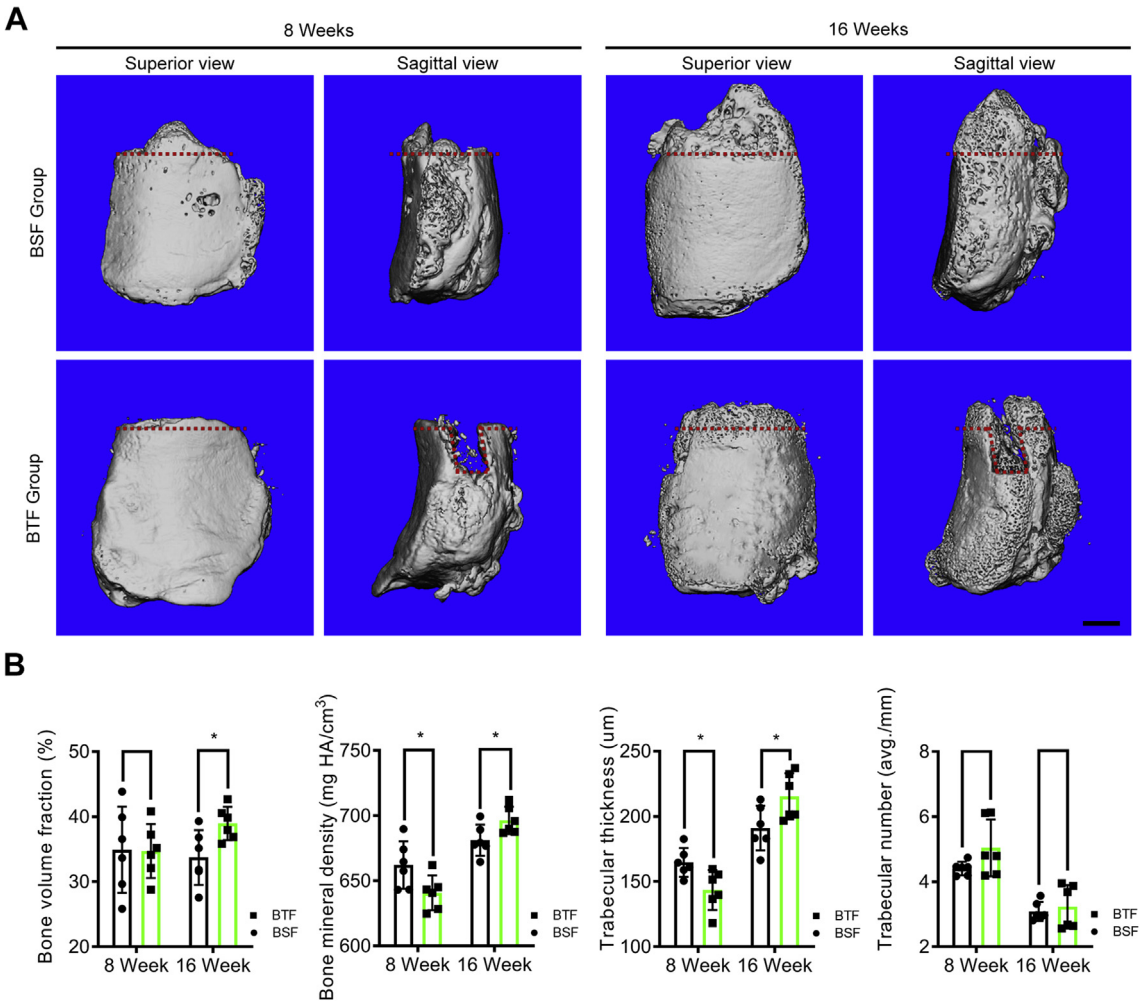

Figure 3. (A) Representative micro-CT images of the proximal patella of the BSF and BTF groups at postoperative week 8 and week 16. The red dotted line indicates the osteotomy site. Scale bar = 1 mm. (B) Comparison of the bone volume fraction (BVF), bone mineral density (BMD), trabecular thickness (Tb.Th) and trabecular number (Tb.N) in newly formed bone between two groups at different time points. *: $p < 0.05$.

BTF groups (Fig. 3). At postoperative 8 weeks, the mean BMD of new bone was 662.14 ± 18.18 mg/cm^3 in the BSF group and 640.79 ± 13.34 mg/cm^3 in the BTF group ($p = 0.04$). The mean Tb.Th of new bone was 164.74 ± 11.04 μm in the BSF group and 143.50 ± 15.28 μm in the BTF group ($p = 0.02$). However, there were no significant differences of the BVF or Tb.N of new bone between the BSF and BTF group. At postoperative week 16, the mean BVF (BTF 38.96 ± 2.54%; BSF 33.73 ± 4.21%), BMD (BTF 696.43 ± 10.52 mg HA/cm^3; BSF 681.26 ± 11.92 mg HA/cm^3) and Tb.Th (BTF 215.48 ± 17.73 μm; BSF 191.13 ± 17.16 μm) of the new bone in the BTF group were significantly higher than those of the BSF group (respectively, $p = 0.03$, $p = 0.04$, $p = 0.04$), but the specimens in the BSF group showed no significant difference in TB.N compared with the specimens in BTF group ($p = 0.64$).

Histological analysis

Histological results showed that new bone was formed at the proximal patella and reattached to the residual patellar tendon by a regenerated fibrocartilage in BSF and BTF groups (Fig. 4). In the BSF group, the tendon to bone interface were filled with cartilage-like tissue and perpendicular bridging fibers. In the BTF group, the fiber alignment ran perpendicular to the base but obliquely at an acute angle to the edge of the bone trough. There seems to be more cartilage-like tissue formed at the base of the bone trough than the edge (Fig. 4). At postoperative week 8, areas of direct bone–tendon reattachment and early fibrocartilage-like tissue formation were observed at the healing site in both groups. Quantitatively, the chondrocyte density of fibrocartilage-like tissue layer in the BTF group was significantly higher than that of the BSF groups ($p < 0.05$), whereas the proteoglycan contents did not show significant difference between the BSF and BTF groups ($p > 0.05$). Moreover, SR staining images captured under polarised microscope indicated that collagen alignment and maturation of the healing tissue in the BTF groups improve significantly with respect to the BSF group ($p < 0.05$) (Fig. 4B). At postoperative week 16, the newly formed bone and regenerated fibrocartilage become more mature, as characterised by well-developed lamellar bone, bone marrow cavities, and transitional fibrocartilage layer. Statistically, the proteoglycan contents in the regenerated fibrocartilage showed significant difference between the BSF and BTF groups ($p < 0.05$). Meanwhile, the BTF group presented significantly better parallel alignment and maturity of collagen fibers in the healing tissue relative to the BSF group ($p < 0.05$). As for the chondrocyte density of fibrocartilage layer, no significant difference was found between the BSF and BTF groups ($p > 0.05$) (Fig. 4B). There were RUNX2 and SOX9 expressions at PPT interface in both groups at week 8 and week 16 (Fig. 5).

Mechanical properties

During tensile testing, all specimens were ruptured at the bone-to-tendon attachment site, and no specimens were excluded. Biomechanical testing showed that the failure load and stiffness increased in the two

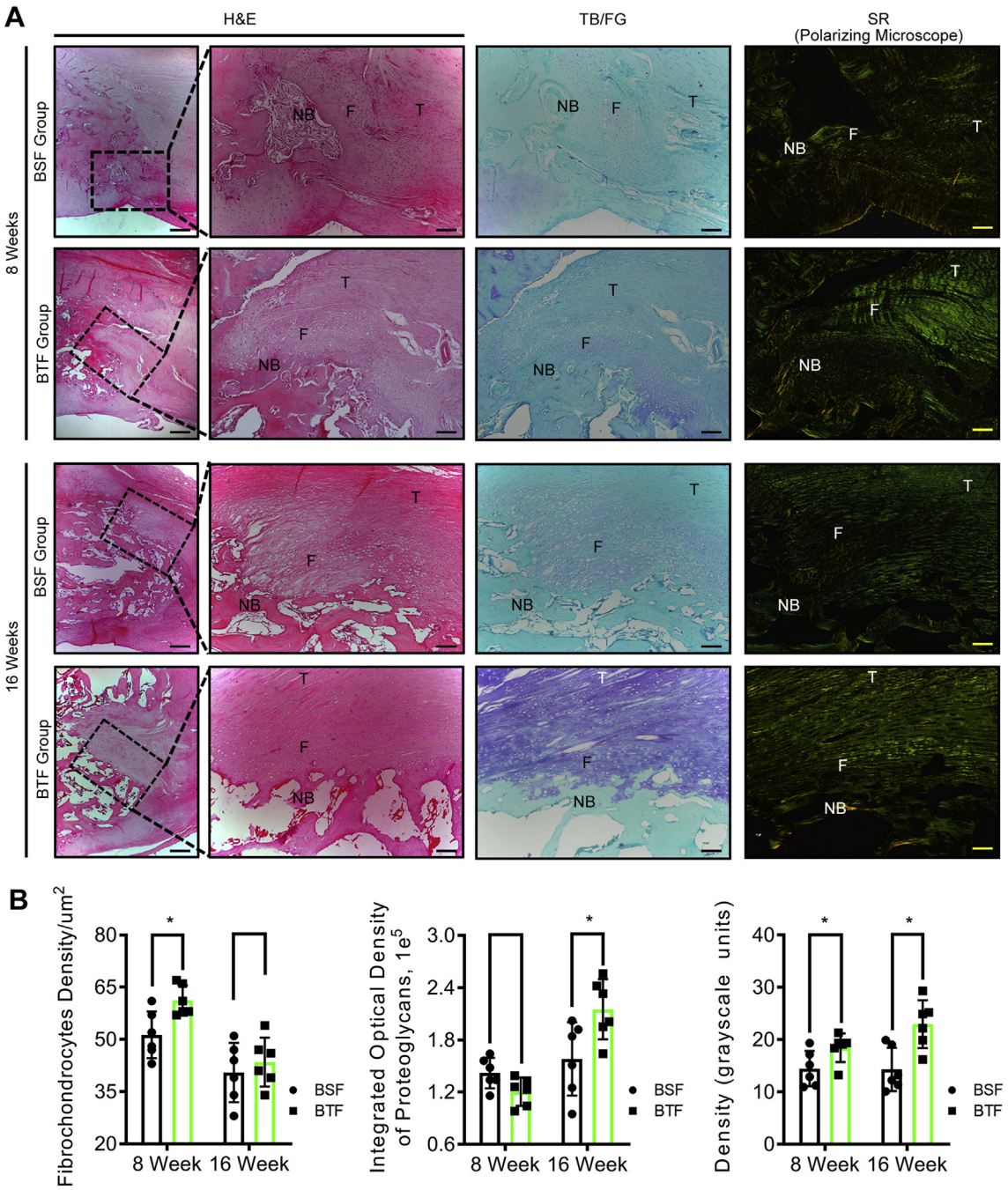

Figure 4. (A) Representative midsagittal sections of the PPT interface of the BSF and BTF groups at postoperative week 8 or 16. Scale bar = 50 μm. (B) Comparison of the fibrochondrocytes density, proteoglycan content, and collagen birefringence between the BSF and BTF groups at postoperative week 8 or 16. *: $p < 0.05$. PPT, patella–patellar tendon; H&E, hematoxylin & eosin; TB, toluidine blue; SR, sirius red; NB, newly formed bone; F, fibrocartilage; T, tendon.

groups from 8 to 16 weeks after operation (Fig. 6B). Statistically, the mean failure load and stiffness of the PPT interface showed no significant difference between the BSF and BTF group at week 8 ($p > 0.05$ for all), whereas the failure load and stiffness of the PPT interface in BTF group were significantly higher than that in BSF group ($p < 0.05$ for all) (Fig. 6B).

Discussion

Surgical integrity is still considered the fundamental therapy for the treatment of BTI injuries [1,3], which can firmly reattach the bone with the ruptured tendon and thus contribute to B–T healing [11,12]. Clinically, the surgical protocols used for B–T reattachment can be categorised into bone surface and trough/tunnel fixations as per the fixation site of the raptured tendon, which causes the B–T healing interface in two absolutely different physical environment [13–16]. However, the effects of the two surgical protocols on B–T healing were confusing. Toward this clinical problem, Silva et al. [16] investigated the effect of bone surface versus trough/tunnel fixation for the repair of flexor digitorum profundus (FDP) tendon insertion site in a canine model. The results indicated that FDP tendon sutured to the cortical surface of distal phalanx was better than sutured to a bone tunnel [16]. However, only the quality of the early repair FDP tendon insertion site was evaluated and the long-term curative effect remained unknown. Recently, a similar research was performed to determine the bone surface versus tunnel fixation for rotator cuff tear in a rabbit model with respect to the histological and

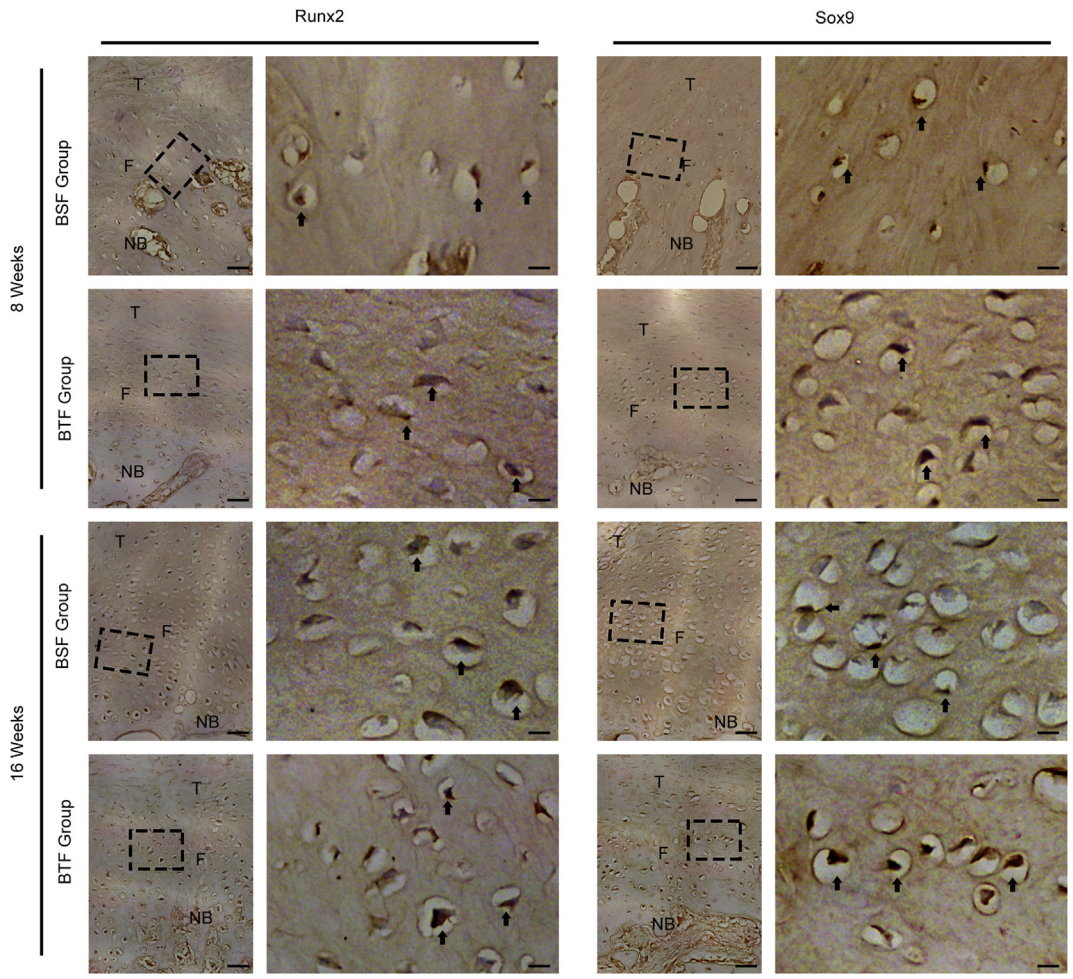

Figure 5. Representative immunohistochemistry of the PPT interface of the BSF and BTF groups at postoperative week 8 or 16. Arrow: positively stained cells. Scale bar = 20 μm (low magnification) or 4 μm (high magnification). PPT, patella–patellar tendon; NB, newly formed bone; F, fibrocartilage; T, tendon.

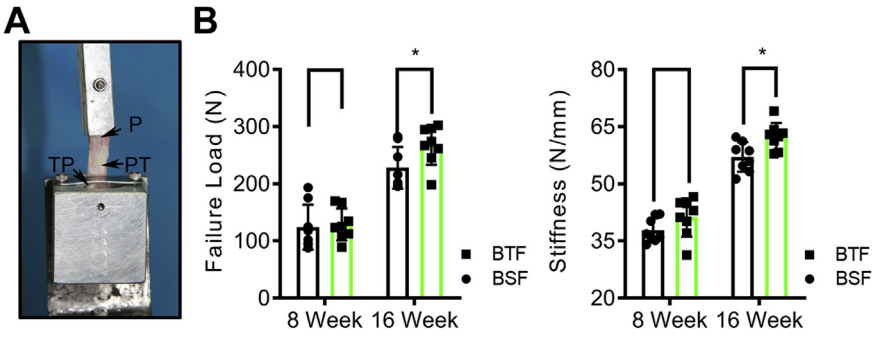

Figure 6. Biomechanical properties of the PPT healing interface. (A) Biomechanical testing of the QPPTC using a custom-made jig that included an upper clamp and a lower clamp to respectively fix the proximal patella and the tibial plateau. (B) The failure load and stiffness of the regenerated PPT interface in BSF and BTF groups at postoperative week 8 or 16. *: $p < 0.05$. PPT, patella–patellar tendon; QPPTCs, quadriceps–patella–patellar tendon–tibia complexes; P, patella; PT, patellar tendon; TP, tibial plateau.

biomechanical properties [19]. The authors demonstrated that BTF for rotator cuff tear showed more fibrocartilage regeneration at the healing interface and higher tissue strength than BSF [19]. But this study did not take the new bone remodelling and mineralisation into consideration. In acxcordance with the previous studies, the B–T healing quality was either influenced by the junctional fibrocartilage regeneration or influenced by new bone remodelling and mineralisation [5,7,20,21]. Only using the fibrocartilage regeneration at the interface to assess B–T healing might be not enough, and new bone remodelling and mineralisation should also be taken into account. Recently, Tan et al. [22] comparatively evaluated the B–T healing between bone tunnel and cortical surface in a rabbit model of biceps tenodesis at postoperative week 8, and their results indicated the two fixation methods were similar in B–T healing quality. Above all, the conclusions in reported literatures are inconsistent, thus, in the present study, a rabbit PPT injury model was designed to compare the long-term effect of bone surface versus trough/tunnel fixations on the B–T healing. The main finding was that a more mature BTI was achieved in the BTF group compared with the BSF group at postoperative week 16, as demonstrated by increased new bone remodelling and mineralisation, mature fibrocartilage regeneration and enhanced biomechanical properties. Thus, the raptured tendon end integrate with bone by BTF was more favorable for B–T healing. This study might provide a valuable reference for the selection of surgical fixation method in the treatment of BTI injury.

In accordance with the previous observations of rabbit PPT healing, no radiographically measurable new bone outgrowth formed at the healing interface of the remaining proximal patella before postoperative 8 weeks [23]. This study was intended to comparatively analyse the effect of bone surface versus trough fixations on the B–T healing for the perspective of new bone mineralisation and remodelling. Thus, the time points selected for analysis should not be early than postoperative 8 weeks. In the present study, the postoperative weeks 8 and 16 were chosen to evaluate the PPT healing quality.

B–T healing underwent the following four typical healing stages: an initial inflammatory stage, a new bone with regenerated fibrocartilage-like layer stage, a woven bone remodelling and maturation of fibrocartilaginous layer stage, and a final remodelling stage [10]. Thus, the importance of fibrocartilage layer regeneration, as well as new bone formation and remodelling for the quality of B–T healing was self-evident. Several literatures have pointed out that the strength of B–T healing was closely connected to the area, length, mineralisation, and BV/TV of new bone [21,24]. Thus, Micro-CT, H&E staining, and RUNX2 expression were used to evaluate the new bone remodelling and mineralisation. At postoperative week 8, micro-CT analysis vividly showed that new bone was obviously extending from the proximal patella in the BSF group, whereas, in the BTF group, only a little new bone formed at the base of patella bone trough. Quantitatively, the BMD and Tb.Th of new bone in the BTF group were lower than that of BSF group, whereas no significant differences in BVF and Tb.N were found between the two groups. Interestingly, at postoperative week 16, the BVF, BMD, and Tb.Th of the new bone in the BTF group were significantly higher than those of the BSF group, but the Tb.N between the BTF and BSF groups still showed no significant difference. In addition, H&E staining further confirmed the differences of new bone remodelling between the BTF and BSF groups. Hence, it is speculated that these variations in new bone remodelling and mineralisation might partly result from the biomechanical property difference between the two groups, as the BVF and mineralisation of new bone were reported to be closely relevant to the biomechanical strength of the PPT interface [21,24]. Unfortunately, the potential cellular and molecular mechanisms about this osteogenic difference were not elucidated in the present study. We thought that the possible mechanism may be the following reasons. In the BTF group, a bone trough was excavated at the residual patella to accommodate the patellar tendon. No doubt the surgical trauma increased, which may perturb the local biological environment more seriously, then consequently influences the new bone remodelling and mineralisation at postoperative 8 weeks [25,26]. As time went by, the local microenvironment becomes more and more similar between the two groups. And, the patellar tendon integrated with residual patella by BTF has a lager contact area with marrow cavity, which could facilitate MSC infiltration and may contribute to new bone remodelling and mineralisation in the BTF group at postoperative week 16.

Functional fibrocartilage is another important component for BTI, which is responsible for the transfer of forces between bony and tendon tissue [27]. The biomechanical functionality of the fibrocartilage is rooted in its histological characterisation, featured by bead-like fibrochondrocytes embedded in an extensive extracellular matrix composed of proteoglycans and collagen [2,27–29]. Therefore, fibrochondrocytes density, proteoglycan content, and collagen alignment were used together as parameters to evaluate fibrocartilage regeneration. Histologically, the PPT healing interface in the BTF group was characterised with better collagen alignment and higher chondrocyte density at week 8. Moreover, the BTF group showed increased proteoglycan content and improved collagen alignment at week 16 compared with that of BSF group. These improvements of fibrocartilage regeneration in the BTF may account for the higher failure load. The fibrocartilage regeneration involves various types of cells including infiltrating inflammatory cells, resident fibroblasts, and tendon or bone marrow–derived MSCs [19,30], and surrounding mechanical cue is a key factor on their migration, proliferation, and differentiation. Mechanical loading is an important element in soft tissue healing. Mechanical loading plays a key role in MSC differentiation. In the BSF group, the interface of the remaining patella was subjected to tensile force acting perpendicular to the interface. The tendon to bone interface were filled with cartilage-like tissue and perpendicular bridging fibers. In the BTF group, the base of the bone trough was subjected to tensile force acting perpendicular to the base. The fiber alignment ran perpendicular to the base but obliquely at an acute angle to the edge of the bone trough. There seem to be more cartilage-like tissue formed at the base of the bone trough than the edge. The different mechanical loadings influence the biological activities of these fibrocartilage regeneration–related cells [31–34] and thus result in the fibrocartilage regeneration variations between the BSF and BTF groups.

Biomechanical testing results indicated that the failure load and stiffness of the repaired PPT interfaces in the BTF group were similar to the BSF group at postoperative week 8, whereas the failure load in the BTF group was significantly higher at postoperative week 16 in comparison with the BSF group. The reasons for this difference at postoperative week 8 may be that the better regeneration of fibrocartilage in the BTF group might have been partly offset by its poor new bone remodelling and mineralisation. Consequently, the BTF group did not display significantly better tensile property than the BSF group. As time went by, the repaired PPT interfaces in the BTF group got better remodelling, characterised by well-developed lamellar bone and regeneration of mature fibrocartilage layer and thus displayed significant improved biomechanical property compared with the BSF group.

Limitations

First, rabbit knee biomechanics and the repair size were absolutely different to human, thus it is not suitable to simply translate our findings into the PPT healing of humans. Second, considering the bone surface and tunnel repair on the early healing of flexor tendon insertion site injuries was previously investigated in a canine model [16], thus we did not study the efficacy difference between the BSF and BTF in early stage of B–T healing. It is possible that the BSF and BTF on early stage of rabbit PPT healing contradicts the aforementioned research preformed in a canine model, and more animal research should be performed to comprehensively and systematically elucidate the impacts of BSF and BTF on B–T healing. Third, in the present study, BTF is more suitable for B–T healing compared with BSF. However, the detail cellular and molecular mechanisms about this were not investigated in the present study. The reason for the phenomenons may be that BTF can provide a stabler mechanical environment and more MSCs for the osteointegration of tendon end with respect to BSF. Fourth, the osteogenic difference should have been affected by the different mechanical loadings between two groups. For sure, the underlying mechanism should be further explored in the future studies.

Conclusions

These results suggested that ruptured tendon fixation in a bone trough resulted in superior B–T healing in comparison with tendon fixation on bone surface in a rabbit PPT injury model.

Fundings

This work was supported by the National Natural Science Foundation of China (81501898).

Conflict of Interest

The authors have no conflict of interest to disclose in relation to this article.

References

[1] Atesok K, Fu FH, Wolf MR, Ochi M, Jazrawi LM, Doral MN, et al. Augmentation of tendon-to-bone healing. J Bone Joint Surg Am 2014;96(6):513–21.

[2] Lu HH, Thomopoulos S. Functional attachment of soft tissues to bone: development, healing, and tissue engineering. Annu Rev Biomed Eng 2013;15:201–26.

[3] Derwin KA, Galatz LM, Ratcliffe A, Thomopoulos S. Enthesis repair: challenges and opportunities for effective tendon-to-bone healing. J Bone Joint Surg Am 2018; 100(16):e109.

[4] Hu J, Qu J, Xu D, Zhang T, Qin L, Lu H. Combined application of low-intensity pulsed ultrasound and functional electrical stimulation accelerates bone-tendon junction healing in a rabbit model. J Orthop Res 2014;32(2):204–9.

[5] Lu H, Chen C, Qu J, Chen H, Chen Y, Zheng C, et al. Initiation timing of low-intensity pulsed ultrasound stimulation for tendon-bone healing in a rabbit model. Am J Sports Med 2016;44(10):2706–15.

[6] Lui P, Zhang P, Chan K, Qin L. Biology and augmentation of tendon-bone insertion repair. J Orthop Surg Res 2010;5:59.

[7] Xu D, Zhang T, Qu J, Hu J, Lu H. Enhanced patella-patellar tendon healing using combined magnetic fields in a rabbit model. Am J Sports Med 2014;42(10): 2495–501.

[8] Leung KS, Chong WS, Chow DH, Zhang P, Cheung WH, Wong MW, et al. A comparative study on the biomechanical and histological properties of bone-to-bone, bone-to-tendon, and tendon-to-tendon healing: an achilles tendon-calcaneus model in goats. Am J Sports Med 2015;43(6):1413–21.

[9] Nebelung W, Becker R, Urbach D, Ropke M, Roessner A. Histological findings of tendon-bone healing following anterior cruciate ligament reconstruction with hamstring grafts. Arch Orthop Trauma Surg 2003;123(4):158–63.

[10] Lu H, Qin L, Cheung W, Lee K, Wong W, Leung K. Low-intensity pulsed ultrasound accelerated bone-tendon junction healing through regulation of vascular endothelial growth factor expression and cartilage formation. Ultrasound Med Biol 2008;34(8):1248–60.

[11] Depres-Tremblay G, Chevrier A, Snow M, Hurtig MB, Rodeo S, Buschmann MD. Rotator cuff repair: a review of surgical techniques, animal models, and new technologies under development. J Shoulder Elb Surg 2016;25(12):2078–85.

[12] Samuelsson K, Andersson D, Ahlden M, Fu FH, Musahl V, Karlsson J. Trends in surgeon preferences on anterior cruciate ligament reconstructive techniques. Clin Sports Med 2013;32(1):111–26.

[13] Hein J, Reilly JM, Chae J, Maerz T, Anderson K. Retear rates after arthroscopic single-row, double-row, and suture bridge rotator cuff repair at a minimum of 1 Year of imaging follow-up: a systematic review. Arthroscopy 2015;31(11): 2274–81.

[14] Slone HS, Romine SE, Premkumar A, Xerogeanes JW. Quadriceps tendon autograft for anterior cruciate ligament reconstruction: a comprehensive review of current literature and systematic review of clinical results. Arthroscopy 2015; 31(3):541–54.

[15] Trudel G, Ramachandran N, Ryan SE, Rakhra K, Uhthoff HK. Supraspinatus tendon repair into a bony trough in the rabbit: mechanical restoration and correlative imaging. J Orthop Res 2010;28(6):710–5.

[16] Silva MJ, Thomopoulos S, Kusano N, Zaegel MA, Harwood FL, Matsuzaki H, et al. Early healing of flexor tendon insertion site injuries: tunnel repair is mechanically and histologically inferior to surface repair in a canine model. J Orthop Res 2006; 24(5):990–1000.

[17] Hao ZC, Wang SZ, Zhang XJ, Lu J. Stem cell therapy: a promising biological strategy for tendon-bone healing after anterior cruciate ligament reconstruction. Cell Prolif 2016;49(2):154–62.

[18] Wang D, Tan H, Lebaschi AH, Nakagawa Y, Wada S, Donnelly PE, et al. Kartogenin enhances collagen organization and mechanical strength of the repaired enthesis in a murine model of rotator cuff repair. Arthroscopy 2018;34(9):2579–87.

[19] Li X, Shen P, Su W, Zhao S, Zhao J. Into-tunnel repair versus onto-surface repair for rotator cuff tears in a rabbit model. Am J Sports Med 2018;46(7):1711–9.

[20] Lu H, Liu F, Chen C, Wang Z, Chen H, Qu J, et al. Low-Intensity pulsed ultrasound stimulation for tendon-bone healing: a dose-dependent study. Am J Phys Med Rehabil 2018;97(4):270–7.

[21] Lu H, Hu J, Qin L, Chan KM, Li G, Li K. Area, length and mineralisation content of new bone at bone-tendon junction predict its repair quality. J Orthop Res 2011; 29(5):672–7.

[22] Tan H, Wang D, Lebaschi AH, Hutchinson ID, Ying L, Deng X-H, et al. Comparison of bone tunnel and cortical surface tendon-to-bone healing in a rabbit model of biceps tenodesis. J Bone Jt. Surg 2018;100(6):479–86.

[23] Qin L, Lu H, Fok P, Cheung W, Zheng Y, Lee K, et al. Low-intensity pulsed ultrasound accelerates osteogenesis at bone-tendon healing junction. Ultrasound Med Biol 2006;32(12):1905–11.

[24] Wen CY, Qin L, Lee KM, Chan KM. Peri-graft bone mass and connectivity as predictors for the strength of tendon-to-bone attachment after anterior cruciate ligament reconstruction. Bone 2009;45(3):545–52. English.

[25] Jayasuriya CT, Chen Y, Liu W, Chen Q. The influence of tissue microenvironment on stem cell-based cartilage repair. Ann N Y Acad Sci 2016;1383(1):21–33.

[26] Miller GJ, Gerstenfeld LC, Morgan EF. Mechanical microenvironments and protein expression associated with formation of different skeletal tissues during bone healing. Biomechanics Model Mechanobiol 2015;14(6):1239–53.

[27] Lu H, Chen C, Wang Z, Qu J, Xu D, Wu T, et al. Characterisation of calcium and zinc spatial distributions at the fibrocartilage zone of bone–tendon junction by synchrotron radiation-based micro X-ray fluorescence analysis combined with backscattered electron imaging. Spectrochim Acta B At Spectrosc 2015;111:15–22.

[28] Moffat KL, Sun WH, Pena PE, Chahine NO, Doty SB, Ateshian GA, et al. Characterisation of the structure-function relationship at the ligament-to-bone interface. Proc Natl Acad Sci USA 2008;105(23):7947–52.

[29] Spalazzi JP, Boskey AL, Pleshko N, Lu HH. Quantitative mapping of matrix content and distribution across the ligament-to-bone insertion. PLoS One 2013;8(9): e74349.

[30] Font Tellado S, Balmayor ER, Van Griensven M. Strategies to engineer tendon/ligament-to-bone interface: biomaterials, cells and growth factors. Adv Drug Deliv Rev 2015;94:126–40.

[31] Gharibi B, Cama G, Capurro M, Thompson I, Deb S, Di Silvio L, et al. Gene expression responses to mechanical stimulation of mesenchymal stem cells seeded on calcium phosphate cement. Tissue Eng A 2013;19(21–22):2426–38.

[32] Xiao E, Yang HQ, Gan YH, Duan DH, He LH, Guo Y, et al. Brief reports: TRPM7 Senses mechanical stimulation inducing osteogenesis in human bone marrow mesenchymal stem cells. Stem Cells 2015;33(2):615–21.

[33] McWhorter FY, Davis CT, Liu WF. Physical and mechanical regulation of macrophage phenotype and function. Cell Mol Life Sci 2015;72(7):1303–16.

[34] Burk J, Plenge A, Brehm W, Heller S, Pfeiffer B, Kasper C. Induction of tenogenic differentiation mediated by extracellular tendon matrix and short-term cyclic stretching. Stem Cell Int 2016;2016. 7342379.